Supplementary Information (SI)

I. Supplementary Figures

II. Supplementary Tables

Supplementary Figures

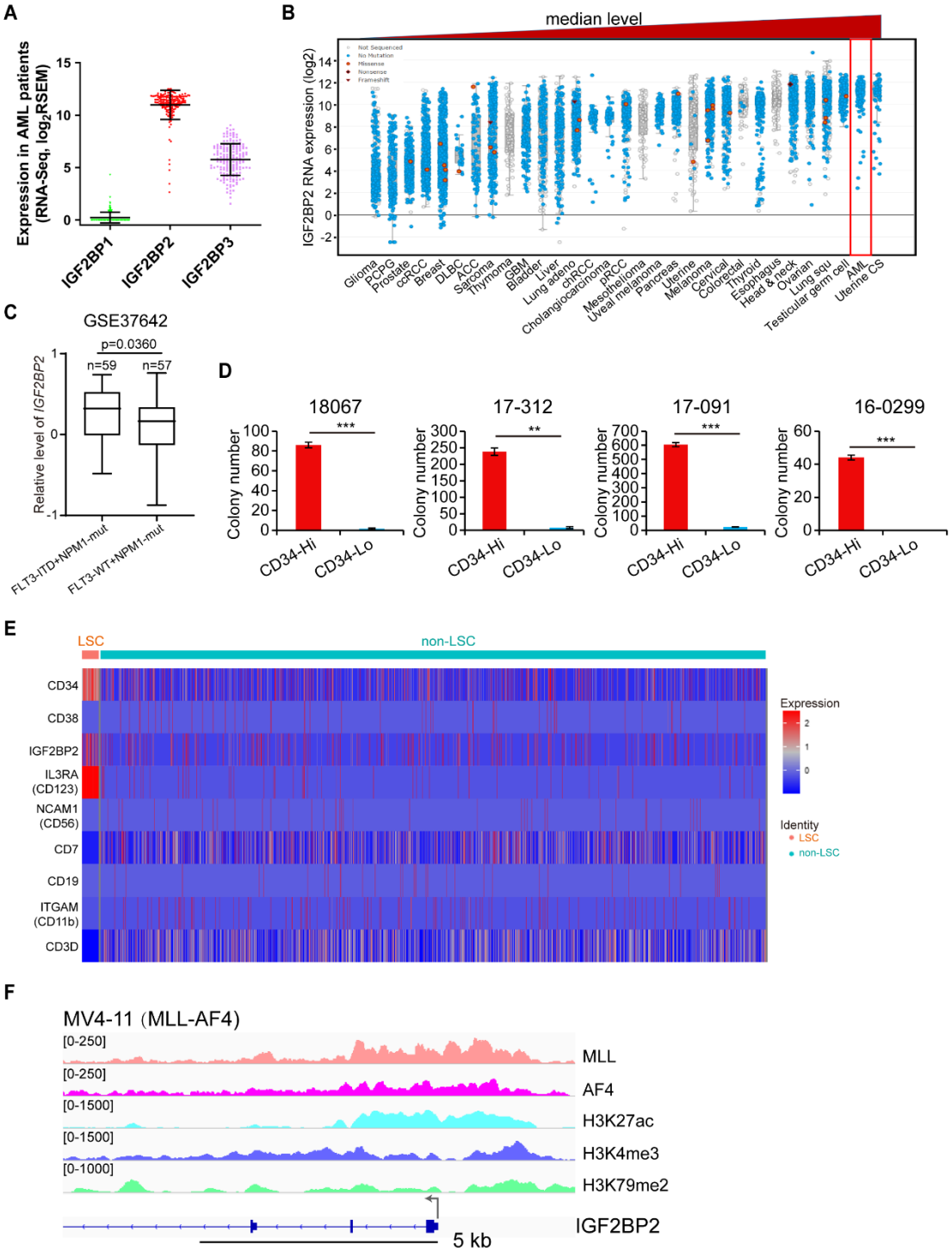

Figure S1 (Related to Figure 1). IGF2BP2 is highly expressed in AML

(A) Relative expression levels of *IGF2BP1*, *IGF2BP2*, and *IGF2BP3* mRNA in AML patients according to the RNA-seq data from TCGA. (B) Expression of *IGF2BP2* in various types of cancer as adopted from cBioPortal for Cancer Genomics (http://www.cbioportal.org/). (C) Comparison of expression levels of *IGF2BP2* in patients with both FLT3-ITD and NPM1 mutations to that in patients with only NPM1 mutation according to the GSE37642 dataset. (D) Colony-forming assays using

mononuclear cells (MNCs) sorted from primary AML patient samples based on the expression of CD34. (E) Heatmap showing expression of *IGF2BP2* and cell surface markers for characterization of LSCs and non-LSCs from scRNA-seq in GSE116481 dataset. (F) IGV tracks showing the binding signal of MLL, AF4, H3K27ac, H3K4me3, and H3K79me2 around TSS of *IGF2BP2* in MV4-11 cells. **p < 0.01; ***p < 0.001; t test.

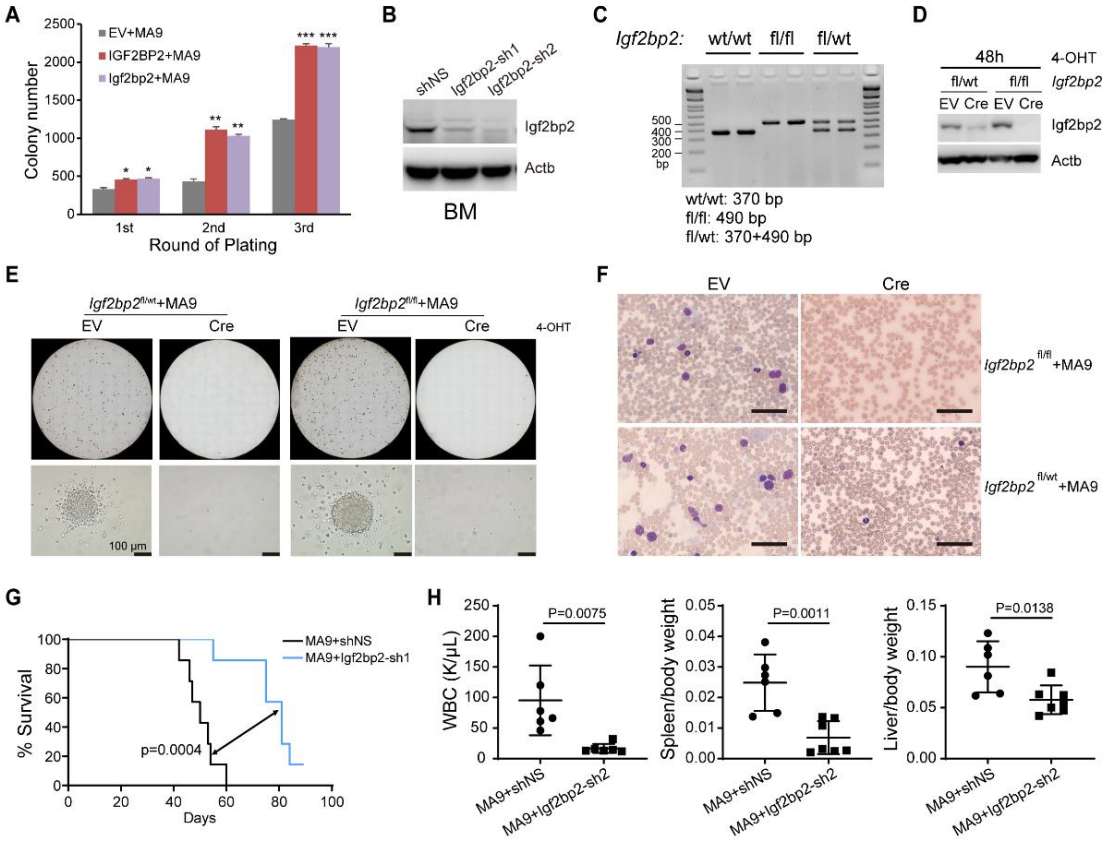

Figure S2 (Related to Figure 2). IGF2BP2 promotes AML initiation/development.

(A) HSPCs collected from wildtype CD45.1 mice were transduced with MSCVneo-MLL-AF9 (MA9) plus MSCV-PIG (EV), MSCV-PIG-IGF2BP2, or MSCV-PIG-Igf2bp2 retroviruses and seeded for CFA. (B) Validation of shRNAs-mediated *Igf2bp2* KD in BM CFA cells by western blot. (C) Genotyping of *Igf2bp2* KO mice. wt, wildtype; fl, flox. (D) Western blot showing knockout of Igf2bp2 in empty vector- (EV) or Cre-infected HSPCs of *Igf2bp2*$^{fl/wt}$ or *Igf2bp2*$^{fl/fl}$ mice upon induction of 4-OHT. Actb was used as a loading control. (E) CFA using mouse HSPCs from *Igf2bp2*$^{fl/wt}$ or *Igf2bp2*$^{fl/fl}$ mice transduced with MA9 plus EV or Cre. 4-OHT was added into the methylcellulose when plating. Photos of the overview wells (upper) or representative colonies (bottom) are shown. (F) Wright–Giemsa staining of PB of the primary BMT recipient mice 5 weeks after transplantation using cells collected from first plating of CFA in Fig. 2E. Bar= 50 μm. (G) Kaplan–Meier curves showing the effect of *Igf2bp2* knockdown on MA9-induced de novo leukemogenesis in lethally irradiated recipient mice. (H) White blood cell (WBC, left), relative spleen weight (middle), and relative liver weight (right) of the primary BMT recipient mice of *Igf2bp2* knockdown at the end point.

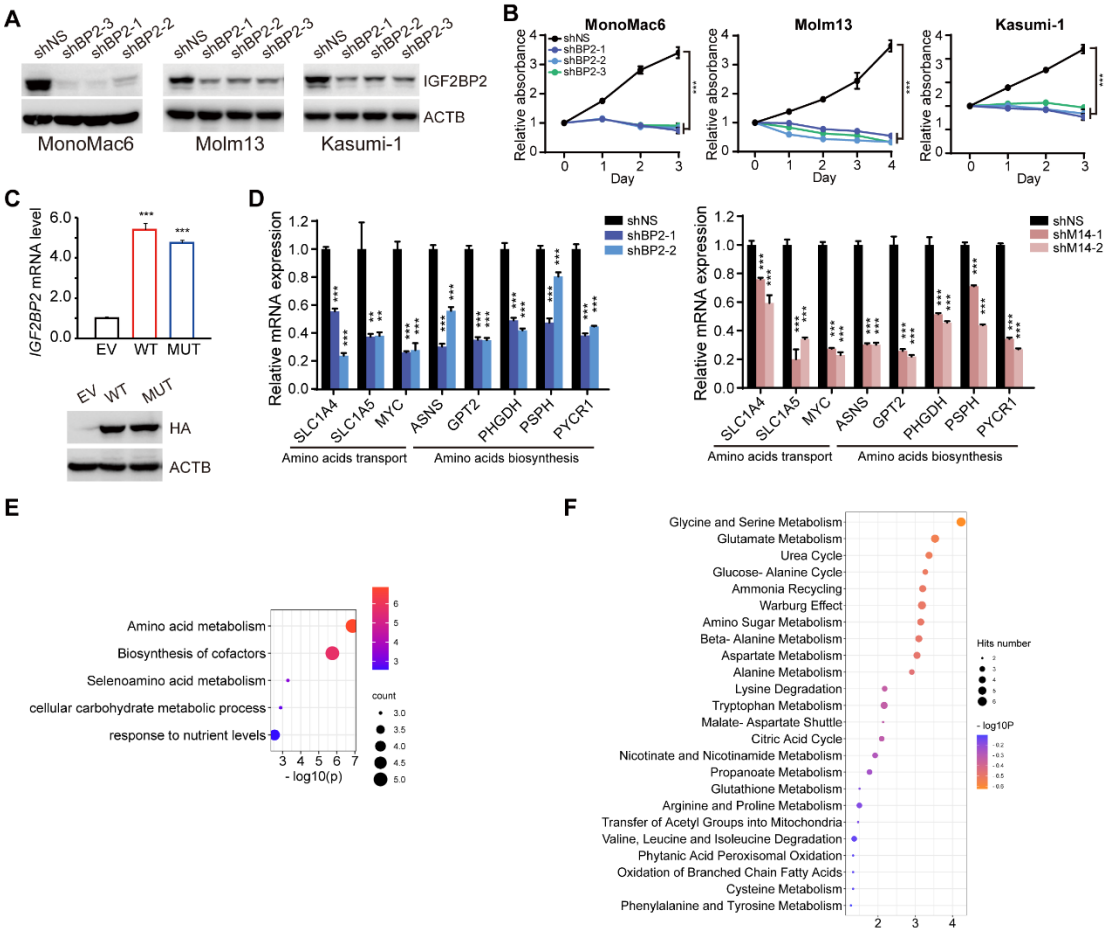

Figure S3 (Related to Figure 3). IGF2BP2 regulates amino acids metabolism in AML cells.

(A) Validation of shRNAs-mediated *IGF2BP2* knockdown in human AML cell lines by western blot. (B) Human AML cell lines were transduced with lentiviral shRNAs targeting human *IGF2BP2* or scramble shRNA (shNS) and seeded for MTT assays. (C) Validation of IGF2BP2 overexpression in MonoMac6 cells transduced with IGF2BP2-WT (WT) or IGF2BP2-KH3-4 mutant (MUT) lentiviruses by qPCR (upper) and western blot (bottom). EV, empty vector. (D) qPCR assays showing decreased expression of representative target genes of *IGF2BP2* in the amino acids transport and biosynthesis pathways upon *IGF2BP2* or *METTL14* knockdown in MonoMac6 cells. (E) Bubble diagram showing enrichment of gene ontology (GO) by the 40 candidate targets of *IGF2BP2* without m^{6}A modification in Fig. 3F. (F) Bubble diagram showing enrichment of metabolic pathways by the metabolites with significantly reduced level in *IGF2BP2*, *METTL3*, *and METTL14* knockdown Kasumi-1 cells.

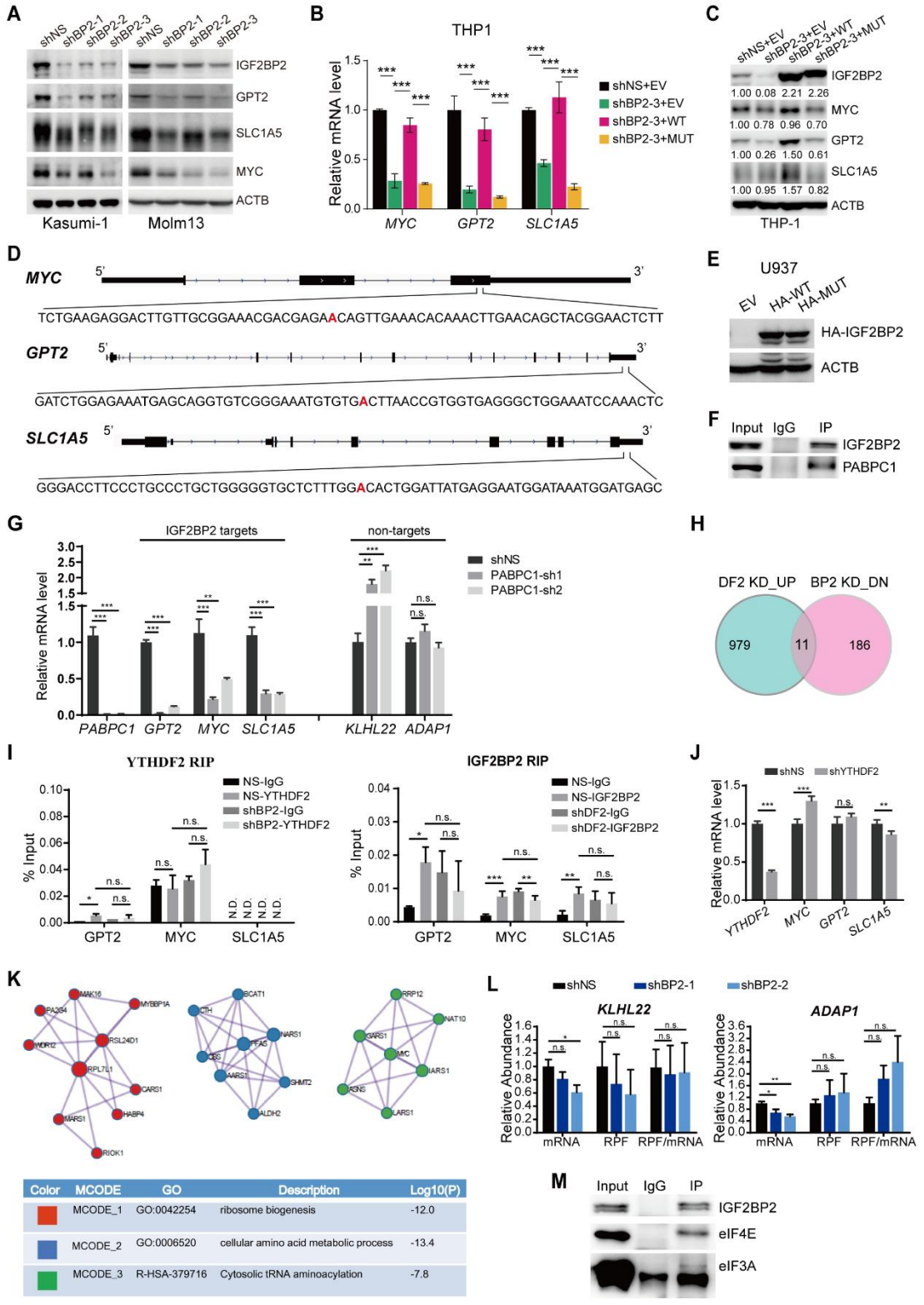

Figure S4 (Related to Figure 4). IGF2BP2 regulates *MYC*, *GPT2*, and *SLC1A5* in an m^{6}A dependent manner.

(A) Western blot showing expression changes of MYC, GPT2, and SLC1A5 after knockdown of *IGF2BP2* in Kasumi-1 and Molm13 cells. (B, C) mRNA (B) and protein

(C) levels of *MYC*, *GPT2*, and *SLC1A5* in *IGF2BP2* knockdown THP1 cells rescued with WT or MUT *IGF2BP2*. (D) High-confidence m^6A sites in the *MYC*, *GPT2*, and *SLC1A5* transcripts. The A bases used for validation by the Bst DNA polymerase-mediated cDNA extension and qPCR assays were highlighted in red. (E) Validation of IGF2BP2 overexpression in U937 cells transduced with IGF2BP2-WT (WT) or IGF2BP2-KH3-4 mutant (MUT) lentiviruses. ACTB was used as a loading control. (F) Co-IP showing interaction of IGF2BP2 and PABPC1 in Molm13 cells. (G) qPCR showing effect of *PABPC1* knockdown on expression of IGF2BP2 target genes (*GPT2*, *MYC*, and *SLC1A5*) and non-target genes (*KLHL22* and *ADAP1*). *ACTB* was used as a reference gene. (H) Venn diagram showing overlapped genes between those upregulated by *YTHDF2* knockdown and downregulated by *IGF2BP2* knockdown. (I) RIP assays using YTHDF2 or IGF2BP2 antibodies were followed by qPCR assays to examine binding of YTHDF2 or IGF2BP2 to *MYC*, *GPT2*, and *SLC1A5* transcripts in Molm13 or MonoMac6 cells, respectively. (J) qPCR showing effect of *YTHDF2* knockdown on expression of *GPT2*, *MYC*, and *SLC1A5*. *ACTB* was used as a reference gene. (K) Molecular Complex Detection (MCODE) algorithm was applied to identify densely connected network components using IGF2BP2 targets genes as input. Pathway and process enrichment of each MCODE component were shown. (L) Relative abundance of *KLHL22* and *ADAP1* mRNA, ribosome protected fragment (RPF), and RFP/mRNA in control (shNS) and *IGF2BP2* knockdown MonoMac6 cells from Ribo-seq. (M) Co-IP showing interaction of IGF2BP2 with eIF4E and eIF3A in Molm13 cells.

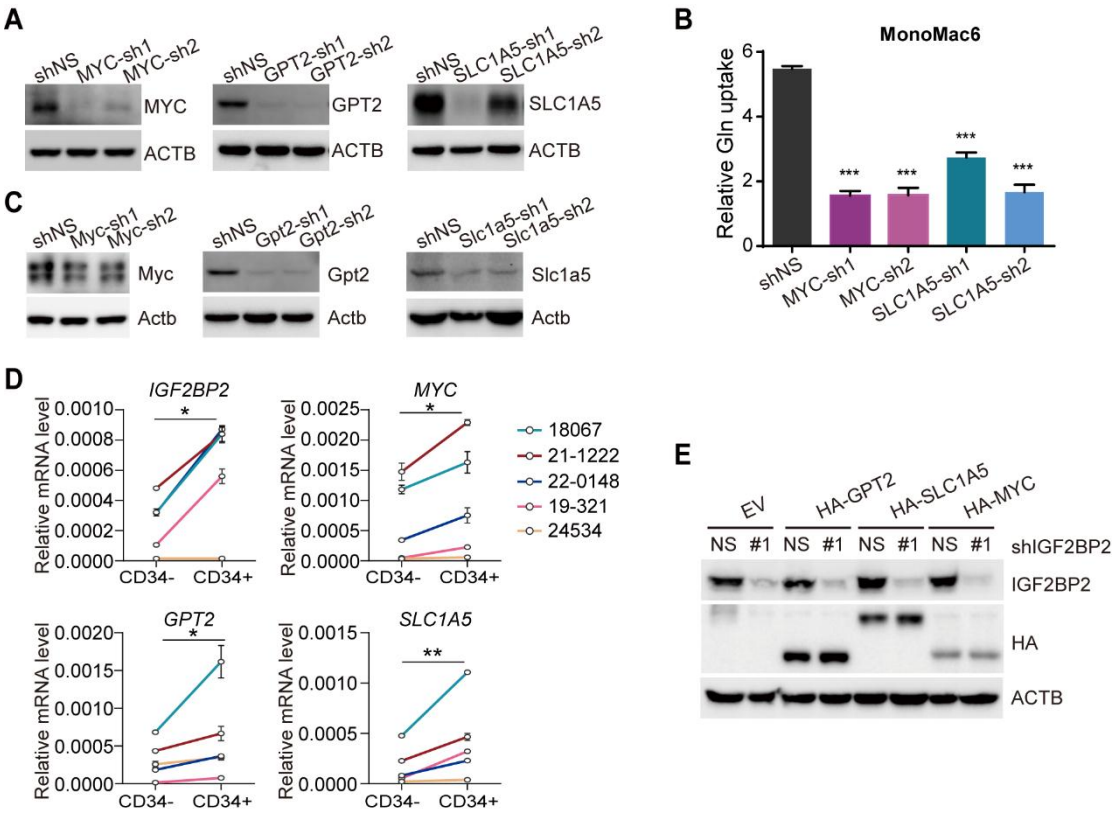

Figure S5 (Related to Figure 5). *MYC*, *GPT2*, and *SLC1A5* are functionally important targets of IGF2BP2.

(A) Validation of shRNAs-mediated knockdown of *MYC*, *GPT2*, and *SLC1A5* in human AML cells by western blot. (B) Effect of depletion of *MYC* or *SLC1A5* on glutamine uptake in MonoMac6 cells. (C) Validation of shRNAs-mediated knockdown of *Myc*, *Gpt2*, and *Slc1a5* in mouse CFA cells by western blot. (D) Expression of *IGF2BP2* and its target genes in CD34+ and CD34- populations from five AML patient samples. (E) MonoMac6 cells were transduced with shNS or IGF2BP2-sh1, and with or without *MYC*, *GPT2*, or *SLC1A5* encoding lentivirus as indicated. Western blots showing knockdown of *IGF2BP2* as well as ectopic expression of *MYC*, *GPT2*, or *SLC1A5* in the corresponding groups.

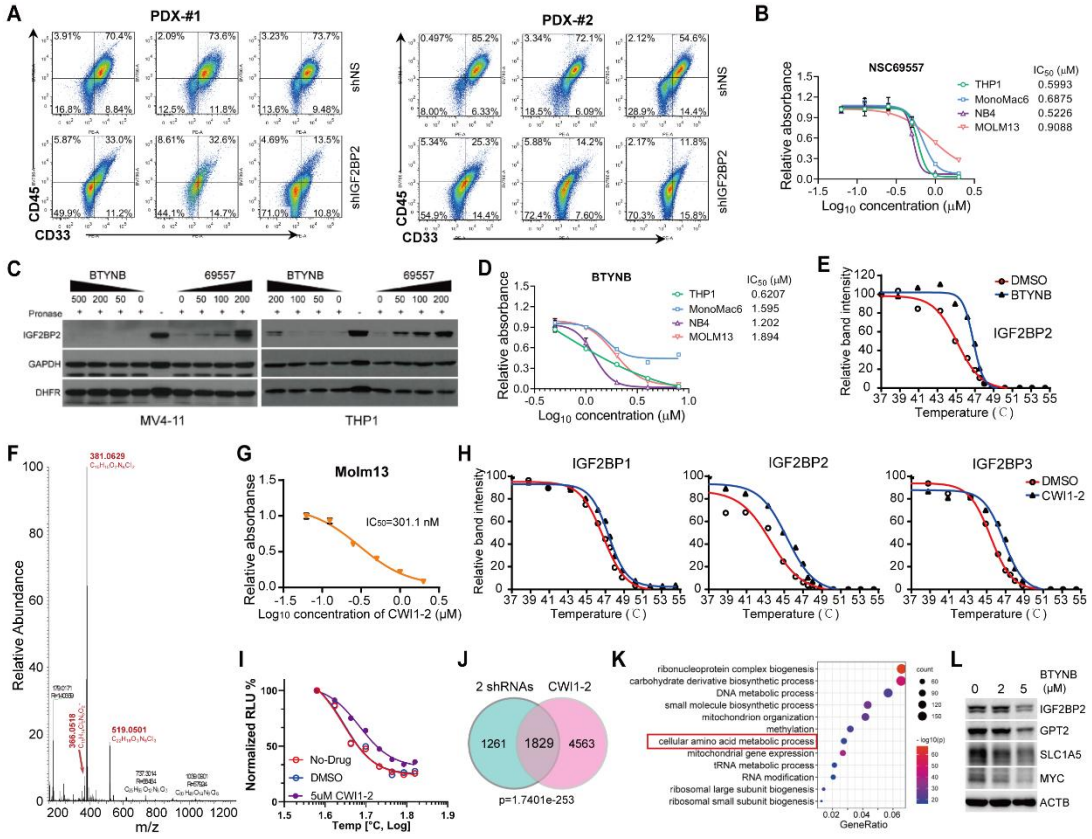

Figure S6 (Related to Figure 6). The therapeutic potential of targeting IGF2BP2 for AML treatment and the identification of CWI1-2 as IGF2BP2 inhibitor.

(A) Engraftment of patient derived AML cells with or with *IGF2BP2* knockdown in the BM of NRGS mice. (B) MTT assays showing the inhibitory effects of NSC69557 from virtual screening on AML cell lines. IC_{50} values after 48 hours of treatment were calculated and shown. (C) DARTS assays comparing the effects of BTYNB and NSC69557 on protecting IGF2BP2 protein in lysates from AML cell lines. (D) MTT assays showing the inhibitory effects of BTYNB on AML cell lines. IC_{50} values after 48 hours of treatment were calculated and shown. (E) Thermal shift curves of IGF2BP2 from CETSA assays in Molm13 pretreated with BTYNB or DMSO. (F) Mass spectrum analysis of the composition of compound NSC69557 obtained from NCI. (G) MTT assays showing the inhibitory effects of CWI1-2 on Molm13 cells. The IC_{50} value after 48 hours of treatment were calculated and shown. (H) Thermal shift curves of IGF2BP1, IGF2BP2, and IGF2BP3 proteins from CETSA assays in Molm13 cell lysates pretreated with 50 μM CWI1-2 or DMSO. (I) Thermal shift curves from IGF2BP2 split-luciferase CETSA assays showing normalized luciferase intensity from 293T cell

lysates treated with 5 μM CWI1-2, DMSO, or no vehicle control (No-drug). (J) Venn diagram showing overlapping of differentially expressed genes (DEGs, FC<0.75 or FC>1.333, P<0.05) by at least 2 shRNAs against IGF2BP2 and CWI1-2 treatment (0.5 μM, 48 hours). The indicated P value was calculated by Fisher's exact test. (K) Bubble diagram showing enrichment of GO pathways by the overlapping downregulated genes by at least 2 shRNAs against IGF2BP2 and CWI1-2 treatment (0.5 μM, 48 hours). (L) Western blot showing effects of BTYNB on the protein level of IGF2BP2, GPT2, SLC1A5, and MYC in Molm13 cells.

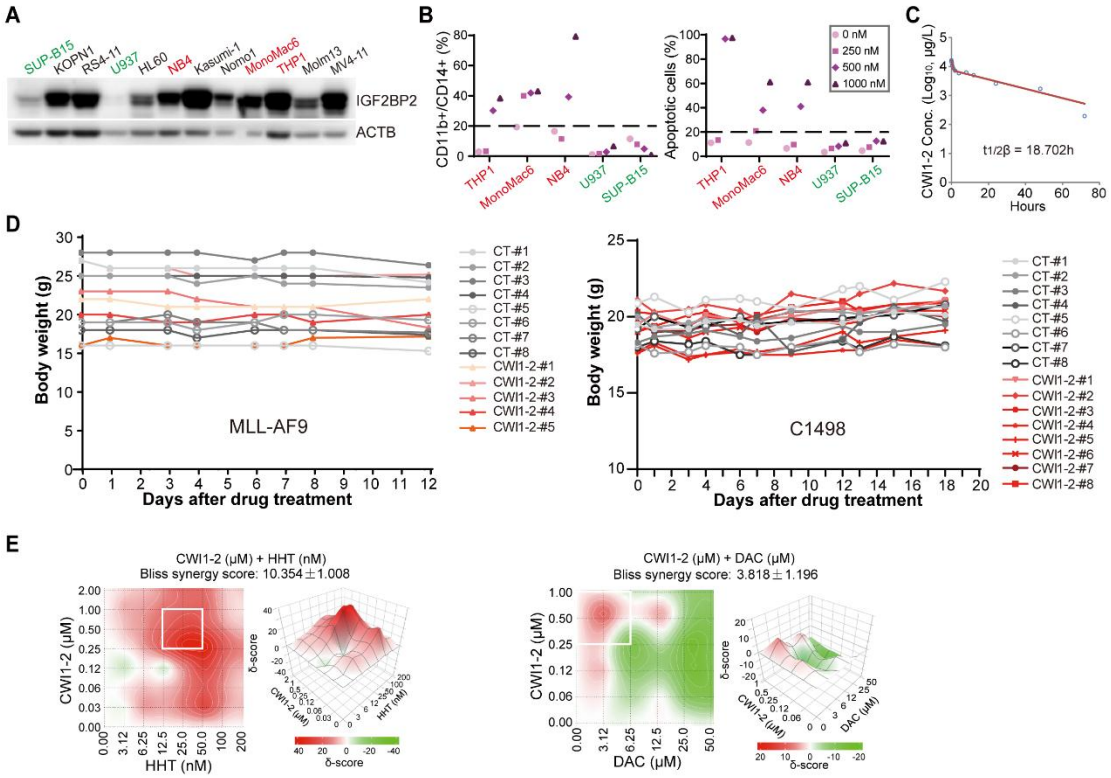

Figure S7 (Related to Figure 7). *In vitro* and *in vivo* efficacy of CWI1-2.

(A) Expression of IGF2BP2 in various AML and ALL cell lines as detected by western blotting. (B) Effect of CWI1-2 on cell differentiation (left) and apoptosis (right) of various AML and ALL cell lines. (C) Pharmacokinetics performed in rats to determine the elimination phase half-life ($t_{1/2}$ β) of CWI1-2 using the two compartment model (R^2 = 0.995). (D) Body weight of BMT recipient mice after i.v. injection of CWI1-2 (5 mg/kg) or vehicle control (CT). (E) Potential synergistic effects of CWI1-2 with homoharringtonine (HHT) or decitabine (DAC) on inhibition of the survival/growth of the C1498 cell line were determined by the Bliss independent model. Drug combinations with the strongest synergistic effects are outlined with white squares. δ-scores represent the percentage of response beyond expectation due to drug interactions.

Supplementary Tables

Table S1 (Related to Figure 1). Patient characteristics and their association with OS (GSE14468)

Characteristic	Patients, N (%)	Events, N (%)	Multivariate analysis	
			HR (95%CI)	*P* Value
Sex				
Female	257(50)	166(65)	1.000	
Male	261(50)	171(66)	0.949(0.764-1.178)	0.634
Age, years				
< 60	446(86)	279(63)	1.000	
⩾60	72(14)	58(81)	1.824(1.354-2.456)	0.000
Median (range)	46(15-77)			
%BM Blast				
< 65	251(48)	157(63)	1.000	
⩾65	267(52)	172(64)	1.142(0.903-1.445)	0.267
Median(range)	65(0-98)			
WBC				
< 28.6	258(50)	162(63)	1.000	
⩾28.6	260(50)	175(68)	1.268(0.998-1.611)	0.052
Median(range)	28.6(0.3-510)			
Platelets				
< 28.6	256(49)	157(61)	1.000	
⩾28.6	262(51)	180(69)	1.153(0.926-1.435)	0.203
Median(range)				
IGF2BP2				
< 0.8	425(82)	266(63)	1.000	
⩾0.8	93(18)	71(76)	1.363(1.036-1.793)	0.027
Flt3-ITD mutation				
negative	378(73)	234(62)	1.000	
positive	140(27)	103(74)	1.567(1.193-2.059)	0.001
Flt3-TKD mutation				
negative	463(89)	309(67)	1.000	
positive	55(11)	28(51)	0.803(0.538-1.197)	0.281
NPM1 mutation				
negative	362(70)	242(67)	1.000	
positive	156(30)	95(61)	0.635(0.486-0.829)	0.001
NRAS mutation				
negative	468(90)	306(65)	1.000	
positive	50(10)	31(62)	0.949(0.642-1.401)	0.791
KRAS mutation				
negative	511(99)	332(65)	1.000	
positive	7(1)	5(71)	2.168(0.878-5.351)	0.093
CEBPA mutation				

negative	480(93)	318(66)	1.000	
positive	38(7)	19(50)	0.563(0.352-0.900)	0.016

Table S2 (Related to Key Resource Table and STAR Methods). List of oligonucleotides

Name	Sequence	Note
GPT2 qPCR-F	CATTCACAGAGGTCATCCGAG	RT-qPCR
GPT2 qPCR-R	GGCACGTTTCTTAGCATCTTC	
SLC1A5 qPCR-F	CCTTTCGCTCATACTCTACCAC	
SLC1A5 qPCR-R	AAACACTACCAAGCCCAGG	
MYC qPCR-F	TTCGGGTAGTGGAAAACCAG	
MYC qPCR-R	AGTAGAAATACGGCTGCACC	
IGF2BP2 qPCR-F	AATCTCTTCATCCCAACCCAG	
IGF2BP2 qPCR-R	ATGACCATCCTTTCGCTGAC	
PABPC1 qPCR-F	GGACCATGAAAAGAAACTTGTGC	
PABPC1 qPCR-R	ACGTTTCCTTGCTCAGTTATCA	
YTHDF2 qPCR-F	CCTTAGGTGGAGCCATGATTG	
YTHDF2 qPCR-R	TCTGTGCTACCCAACTTCAGT	
Igf2bp2 qPCR-F	CAATCCATGCTACCCCAGAAG	
Igf2bp2 qPCR-R	TGCCAATCAGTCTTCCAACG	
ACTB qPCR-F	CACTCTTCCAGCCTTCCTTC	
ACTB qPCR-R	GTACAGGTCTTTGCGGATGT	
18S rRNA qPCR-F	GTAACCCGTTGAACCCCATT	
18S rRNA qPCR-R	CCATCCAATCGGTAGTAGCG	
GPT2-Bst-PCR-F2	TGACCAGGGTTCTCTGAATCTG	BST-qPCR
GPT2-Bst-RT-NT2	CATTTCCCGACACCTGCTC	
GPT2-Bst-RT-m6A	AGCCCTCACCACGGTTAAG	
SLC1A5-Bst-PCR-F	CACTGAGGAAGGAAACCC	
SLC1A5-Bst-RT-NT	CCAGAGCCCTAGCTCAT	
SLC1A5-Bst-RT-m6A	CATTTATCCATTCCTCATAATCCAGTG	
MYC-Bst-PCR-F	GTGACCAGATCCCGGAGTTG	
MYC-Bst-RT-NT	TTGCTCCTCTGCTTGGACG	
MYC-Bst-RT-m6A2	AGCTGTTCAAGTTTGTGTTTCAACTG	
GPT2- F	AGAAATGAGCAGGTGTCGGG	meRIP-qPCR and RIP-qPCR
GPT2- R	TTCACACCGCTAAGGGCTTT	
SLC1A5- F	CCTCACTCTGGCCATCATCC	
SLC1A5- R	CCCAGAGCGTCACCTTCTAC	
MYC- F	GCATACATCCTGTCCGTCCA	
MYC- R	GTCGTTTCCGCAACAAGTCC	

ss-m6A	5'biotin-CGUCUCGG(m6A)CUCGG(m6A)CUGCU-3'	RNA oligos for RNA pulldown
MYC-m6A	5'biotin-GAAGAGG(m6A)CUUGUUGCGGAAACGACGA GA(m6A)CAGUU-3'	
GPT2-m6A	5'biotin-GAAATGTGTG(m6A)CTTAACCGTG-3'	
SLC1A5-m6A	5'biotin-TGCTCTTTGG(m6A)CACTGGATTA-3'	